ISRM Suggested Method for the Needle Penetration Test

Resat Ulusay, Ömer Aydan, Zeynal A. Erguler, Dominique J. M. Ngan-Tillard, Takafumi Seiki, Wim Verwaal, Yasuhito Sasaki, and Akira Sato

1 Introduction

Estimation of mechanical properties of intact rock is usually required for assessment of the stability of rock structures. They are also important elements of the rock classifications used in empirical assessment of rock masses. Measurement of these properties requires laboratory testing, which must be performed on samples of certain dimensions to fulfill testing standards and/or suggested methods. Laboratory tests are also time-consuming due to sample preparation, as well as experimental procedures often require high-capacity loading devices. High-quality core samples recommended by standards and/or suggested methods for the laboratory tests cannot always be obtained, particularly from weak and clay-bearing rocks. For these reasons, some simple and inexpensive index test methods have been developed to indirectly estimate the mechanical properties of intact rock (ISRM 2007). However, even preparation of smaller samples from weak and clay-bearing rocks for some index tests is still troublesome. In addition, geo-engineering and/or restoration studies on natural and man-made historical rock structures and monuments or buildings built with masonry construction techniques may require the determination of mechanical properties of intact rock. Sampling from such ancient sites is not allowed due to preservation, and environmental and other concerns resulting in the lack of mechanical data for those studies.

To overcome the above-mentioned difficulties, a portable, lightweight and non-destructive testing device, called needle penetrometer, was developed in Japan and released as a suggested method by the Rock Mechanics Committee of the Japan Society of Civil Engineers (JSCE-RMC 1980). Similarly, Public Works Research Institute (PWRI 1987) published a draft manual of the test for weak rock mass classification of dam foundation. In the following years, JSCE (1991) revised the suggested method. Recently, JGS (2012) published the JGS standard for the needle penetration test, JGS 3431-2012.

According to the suggested method of Japan Society of Civil Engineers (JSCE 1991) and JGS (2012), the needle penetration test is applicable to soft rocks having uniaxial compressive strength (UCS) less than about 9.8 MPa.

The needle penetration test is a non-destructive index test applicable both in the field and laboratory to determine the needle penetration index (NPI) and does not require any

Please send any written comments on this ISRM Suggested Method to Prof. Resat Ulusay, President of the ISRM Commission on Testing Methods, Hacettepe University, Department of Geological Engineering, 06800 Beytepe, Ankara, Turkey.

Originally published as an article in the journal Rock Mechanics and Rock Engineering, 47, R. Ulusay, Ö. Aydan, Z. A. Erguler, D. J. M. Ngan-Tillard, T. Seiki, W. Verwaal, Y. Sasaki, A. Sato, ISRM Suggested Method for the Needle Penetration Test, 1073–1085, 2014.

R. Ulusay (✉)
Department of Geological Engineering, Hacettepe University, Ankara, Turkey
e-mail: resat@hacettepe.edu.tr

Ö. Aydan (✉)
Department of Civil Engineering and Architecture, University of the Ryukyus, Okinawa, Japan
e-mail: aydan@tec.u-ryukyu.ac.jp

Z. A. Erguler
Department of Geological Engineering, Dumlupınar University, Kutahya, Turkey

D. J. M. Ngan-Tillard · W. Verwaal
Department of Geoscience and Engineering, Delft University of Technology, Delft, The Netherlands

T. SeikiDepartment of Architecture and Civil Engineering, Utsunomiya University, Utsunomiya, Japan

Y. Sasaki
Public Works Research Institute, Geology Research Team, Tsukuba, Japan

A. Sato
Graduate School of Science and Technology, Kumamoto University, Kumamoto, Japan

R. Ulusay (ed.), *The ISRM Suggested Methods for Rock Characterization, Testing and Monitoring: 2007–2014*, DOI: 10.1007/978-3-319-07713-0,

special sample preparation. Several correlations between NPI values and other physico-mechanical properties of intact rock have been established by several authors for a number of rock types. The NPI value is mainly used to estimate the UCS of intact rock (e.g., Okada et al. 1985; Yamaguchi et al. 1997; Takahashi et al. 1988; Uchida et al. 2004; Aydan et al. 2006, 2008; Aydan 2012; Erguler and Ulusay 2007; Park et al. 2011; Ulusay and Erguler 2012). However, its use was also extended to allow assessing of other physico-mechanical properties of intact rock such as tensile strength, Young's modulus and P-wave velocity from NPI (Aydan 2012; Aydan and Ulusay 2013). Aydan et al. (2013) included also cohesion, friction angle and S-wave velocity in addition to the parameters previously covered by Aydan (2012). It should be stressed that that these correlations, though very helpful, comprise a high scatter. So, they are not intended to entirely replace proper evaluation of the aforementioned properties, but to easily provide estimates of their values.

The needle penetration test described in this suggested method is applied to rock specimens and rock exposures to determine the needle penetration index (NPI). In this suggested method, the device and operating procedure are described together with data evaluation. Documentation and presentation of the results are also explained. In addition, all possible uses of the NPI in practice, and other issues related to NP test such as rate of penetration, the effect of needle geometry, influence of grain size, degree of micro structural damage by needle, effect of water, variation of NPI with freezing–thawing and drying–wetting cycles and the possible use of different needle types are also presented in the last section.

2 Scope

The needle penetration test can be performed in the field on rock exposures or in laboratory on rock specimens. It uses a light portable device, called needle penetrometer that pushes a needle into the rock.

The needle penetration test is intended for the determination of the needle penetration index (NPI). This index value can be used to estimate other physico-mechanical properties of intact rock with which NPI is correlated, for example UCS.

3 Testing Device

The needle penetrometer (NP), a lightweight portable device (about 600–700 g), is used to make a needle penetrate into a rock surface (Fig. 1). The needle is a hardened steel, 0.84-mm-diameter rod terminated by a conical tip (Fig. 2). It is a sewing needle designated as JIS S 3008 (No. 2).

The device mainly consists of presser, chuck, penetration scale (0–10 mm, 1 mm graduation), load scale (0–100 N, 10 N graduation), load indicator ring, cap (removable; spare

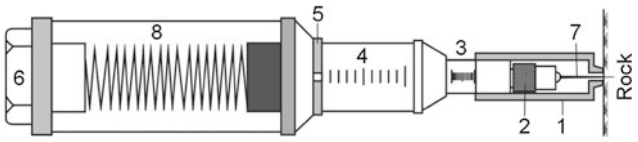

Fig. 1 Needle penetrometer and its parts: *1* presser, *2* chuck, *3* penetration scale, *4* load scale, *5* load indicating ring, *6* cap, *7* penetration needle and *8* spring

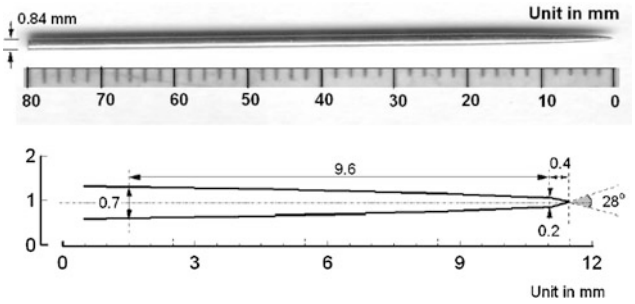

Fig. 2 Sewing needle designated as JIS S 3008 (No. 2) and its geometry (Aydan et al. 2013)

penetration needles contained in the grip), penetration needle and spring mounted in the penetrometer grip as shown in Fig. 1. To insert the needle, the presser (Fig. 1, part 1) is removed from the penetration scale (Fig. 1, part 3) using the vertical and horizontal notches, the chuck (Fig. 1, part 2) is turned counterclockwise and the penetration needle is inserted. Then the chuck is turned clockwise for fastening and fixing the needle and the presser is set using the co-axial notch for zero point adjustment of the penetration scale. The split-type load indicator ring (Fig. 1, part 5) is adjusted manually to zero. The device can measure the applied load up to 100 N and the penetration depth is up to 10 mm.

Based on data from needle penetration tests obtained from literature (i.e., Okada et al. 1985; Aydan 2012; Aydan et al. 2006, 2008, 2013; Erguler and Ulusay 2007; JSCE-RMC 1980; Takahashi et al. 1988; Yamaguchi et al. 1997; Ulusay and Erguler 2012), although this test has been used for rocks with UCS up to 35 MPa, it is generally recommended that it should be used for rocks with UCS lower than 20 MPa, in order to obtain realistic results the penetration of the needle should be more than 1 mm without causing any damage to the needle (Fig. 3).

4 Procedure

The needle penetrometer (NP) device can be used both on rock exposures in the field and on specimens with cylindrical, cubic or prismatic shapes prepared from cores or blocks. It does not require any special preparation of the rock surfaces or specimens. However, before testing, if the surface on which the test will be performed shows some

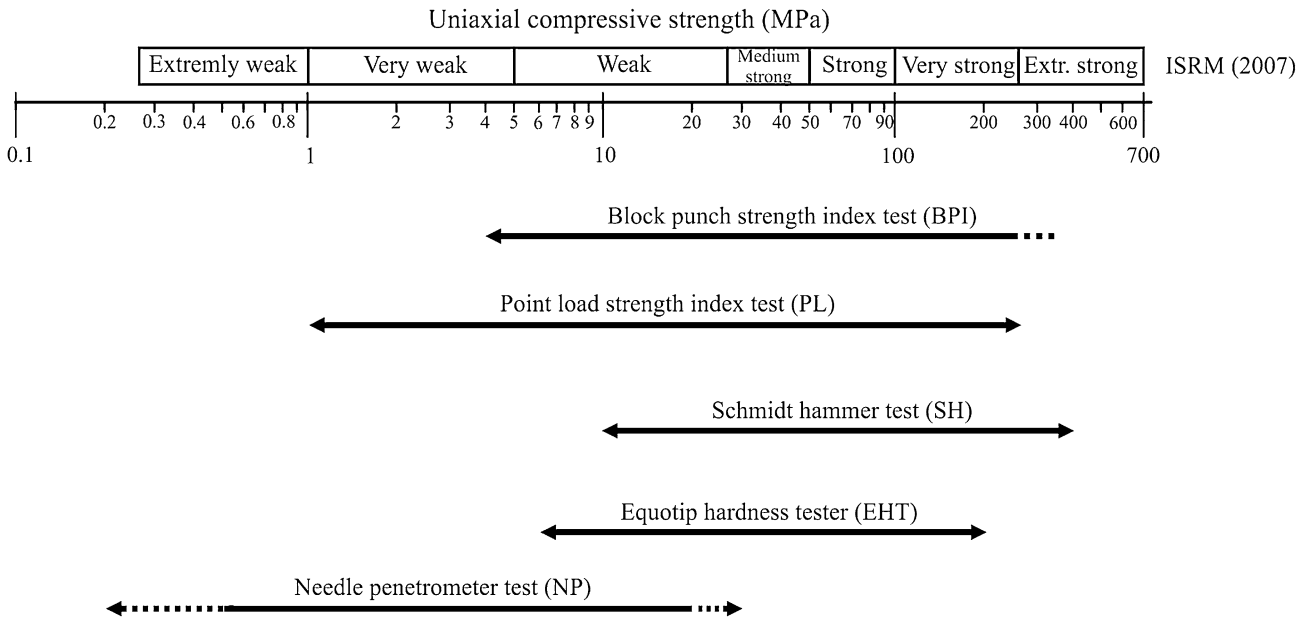

Fig. 3 Ranges of applicability of the most commonly used index tests in rock engineering and the needle penetration test for estimating the UCS (Ulusay and Erguler 2012)

asperities, they have to be removed. Since the test is only intended for weak/soft rocks, they can easily be grinded using common instruments such as files, sandpaper or pocketknives.

The size of samples should be such that no splitting of some samples occurs. Based on the experience, splitting may occur in laboratory samples having a size of 35 × 35 × 35 mm. Therefore, sample size is suggested to be about 40 × 40 × 40 mm for prismatic samples and 40–50 mm in diameter for cylindrical samples having a height greater than 15 mm. The NP test can be used in any direction.

The test is performed by holding tightly the truncated conical joint between load and displacement graduations with one hand and the main body with the other hand, and slowly pushing manually the penetrometer needle into the rock surface or specimen as shown in Fig. 4a, b. The load should be applied perpendicularly to the surface. It is recommended that users hold the needle penetrometer always in the same position, i.e., with both hands. It should be noted that if the operator becomes less focused and starts changing his/her usual modus operandi (e.g., holding the penetrometer with just one hand), the scattering of the NPI values will increase.

The needle is pushed into the rock until 100 N is reached; at this stage the penetration depth is measured from the position of the presser on the penetration scale (Fig. 1, part 3). Then, the needle is slowly pulled out. With softer and saturated rocks, it is possible that, before the maximum penetration force is reached, the maximum penetration depth (10 mm) is attained. In this case, the test stops at this depth, the penetration load is read from the load scale (Fig. 1, part 4) and the needle is slowly pulled out.

The test is repeatedly carried out on the same surface between three to five times. However, if the results are not consistent or too scattered, the number of tests can be increased. At each time, the penetration point of the needle is shifted by at least 10 mm from the previous point.

During penetration, some fractures may develop and may create a radially fractured zone. It should be noted that when the needle is withdrawn, some inverted cones and associated fractures may also develop. If fractures develop during the penetration procedure, the results of such tests should be discarded (Fig. 5). However, if such fractures develop during the withdrawal of the needle, the test can be accepted as valid. In addition, if needle penetration causes tensile splitting of the specimen along a weakness plane, such as bedding or schistosity, the test should also be discarded.

5 Calculations

The needle penetration index (NPI) is calculated from the following equations:

$$\text{for } F = 100 \text{ N and } D \leq 10 \text{ mm}, \quad \text{NPI} = 100/D \tag{1a}$$

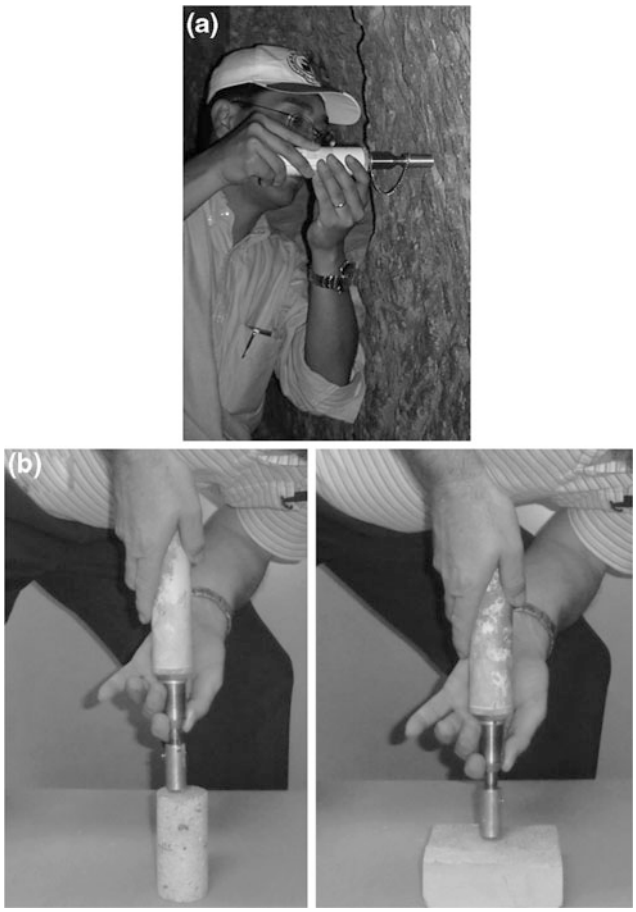

Fig. 4 Application of the needle penetrometer in **a** field on a rock exposure and **b** laboratory on core and prismatic samples

$$\begin{aligned} &\text{for } D = 10 \text{ mm and } F < 100 \text{ N} \\ &\text{NPI} = F/10 \text{ (for } F \leq 100 \text{ N)} \end{aligned} \quad (1b)$$

where F is the applied load (N) and D is the depth of penetration (mm). The unit of NPI is N/mm.

The values of the NPI should be <100 N/mm and >1 N/mm, as the minimum graduation of the penetration scale is 1 mm and that of the load scale is 100 N.

The mean of the NPI values calculated using at least three points of measurement on the same testing surface is taken as the NPI value of the specimen or rock exposure.

Though the effect of the needle penetration rate on the NPI is negligible, each test should take around 30 s to perform.

In certain types of rocks displaying grain or porosity heterogeneity at the scale of the needle diameter (e.g., grains larger than 10 mm, uneven distribution of pores or a mixture of crushable with less crushable grains), a large scatter of the NPI values is expected. In the case of rocks with coarse hard grains in a soft cementing material, such as breccia or conglomerate, the NP test can be cautiously used to infer the properties of the soft matrix.

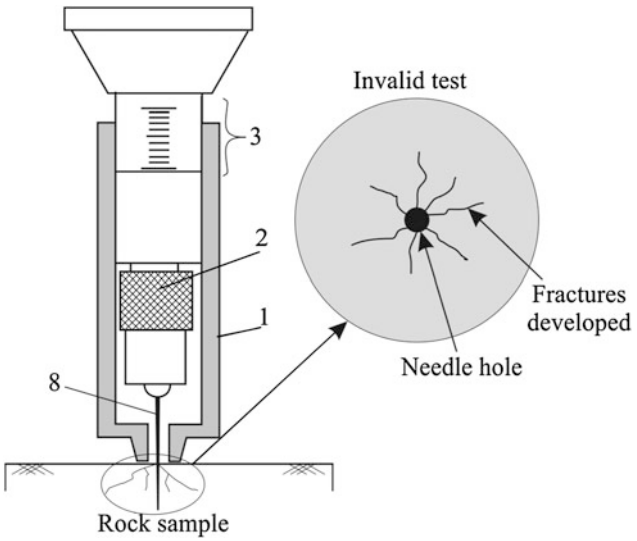

Fig. 5 Schematic illustration of an invalid NP test (Ulusay and Erguler 2012)

6 Reporting of Results

The report should contain at least the following information for each tested specimen or rock exposure:

(a) Lithological description of the rock.
(b) Orientation of the direction of penetration with respect to specimen anisotropy, e.g., bedding planes, schistosity, etc. (in degrees).
(c) Type of laboratory specimen or rock exposure.
(d) Identification of the laboratory specimen with sample number, source location and sampling depth and date, or identification of the rock exposure with description of the site.
(e) Number of tested specimens or rock exposures.
(f) Water content at the time of test (air dried, oven dried or value of water content in percent).
(g) Date of testing.
(h) A tabulation of the values of applied load and depth of penetration at each application point on the rock surface and the calculated mean NPI value.

7 Technical Issues Regarding Needle Penetration Test

The non-destructive nature of the NP test and the limited requirement for specimen preparation make it possible to perform both in laboratory and field. In addition, in geoengineering or restoration studies conducted at historical rock structures or sites, where rock sampling for laboratory strength determinations is not allowed, the NP test can also

Table 1 Examples of empirical prediction equations to infer some mechanical properties of rocks from NPI*

Rock material property	Equation	Recommended by	Rock types tested
Uniaxial compressive strength, σ_c	σ_c (MPa) = 0.4 NPI$^{0.929}$ (N/mm)	Ulusay and Erguler (2012)	Marl, tuff, mudstone, siltstone, sandstone, greywacke, very stiff clay; data from Japan
	σ_c (MPa) = 0.2 NPI (N/mm)	Aydan (2012)	Tuff, sandstone, pumice, limestone, lignite measures (lignite, mudstone, siltstone, marl, loam)
	σ_c (kPa) = 27.3 NPI + 132 (N/cm)	Uchida et al. (2004)	Sandstone
	log σ_c (kgf/cm^2) = 0.978 log NPI + 1.599 (kgf/mm)	Okada et al. (1985)	Artificial cement-based samples and mudstone
	σ_c (MPa) = 1.539 NPI$^{0.9896}$ (N/mm)	Takahashi et al. (1988)	Sandstone, mudstone, conglomerate, greywacke, tuff
	log σ_c (kgf/cm^2) = 0.982 logNPI-0.209	Yamaguchi et al. (1997)	Pyroclastic flow and fall deposits
Tensile strength, σ_t (MPa)	σ_t = 0.02 NPI (NPI, N/mm)	Aydan (2012)	Tuff, pumice, lignite measures (lignite, mudstone, siltstone, marl, loam)
Young's modulus, E_i (GPa)	E_i = 0.05 NPI (NPI, N/mm)	Aydan (2012)	Tuff, sandstone, pumice, limestone, soapstone, lignite measures (lignite, mudstone, siltstone, marl, loam)
P-wave velocity, V_p (km/s)	V_p = 0.33 + 0.3 NPI$^{0.5}$ (NPI, N/mm)	Aydan (2012)	Tuff, sandstone, soapstone, pumice limestone, lignite measures (lignite, mudstone, siltstone, marl, loam)
Cohesion, c (MPa)	c = 0.04 NPI (NPI, N/mm)	Aydan et al. (2013)	Tuff, sandstone, soapstone, pumice limestone, lignite measures (lignite, mudstone, siltstone, marl, loam)
Friction angle ϕ (°)	ϕ = 54.9 (1 − exp(−NPI/10) (for tensile stress regime)	Aydan et al. (2013)	Tuff, sandstone, soapstone, pumice limestone, lignite measures (lignite, mudstone, siltstone, marl, loam)
	ϕ = 13.375 NPI$^{0.25}$ (for compressive stress regime) (NPI, N/mm)		
S-wave velocity, V_s (km/s)	V_s = 0.1 + 0.18 NPI$^{0.5}$ (NPI, N/mm)	Aydan et al. (2013)	Tuff, sandstone, soapstone pumice limestone, lignite measures (lignite, mudstone, siltstone, marl, loam)

* The diameter of the needle is 0.84 mm. Lignite measures of rocks are given in parentheses

be effectively used to provide estimates of the rock strength as well as other geomechanical properties.

This section summarizes a series of research studies addressing several technical issues regarding the tests, such as the correlations established with other rock strength parameters, the influence of some particular details and conditions of the tests, e.g., grain size, needle geometry and penetration rate, micro structural damage, environmental aspects (water content, freeze–thaw and wet–dry cycles), and relaxation and creep.

7.1 Correlations with Other Geomechanical Parameters and Estimation of the Weathering Degree

Several authors have presented results from their researches concerning the potential use of the needle penetration test to estimate other rock strength parameters, such as uniaxial compressive strength, Young's modulus, tensile strength and elastic wave velocity, and shear strength parameters.

In Table 1, a wide variety of correlations are presented. It is strongly recommended to consult the original references before using the estimates they provide, to confirm that they can be applied and to assess the respective dispersions.

7.1.1 Correlations with Other Geomechanical Parameters

Empirical relationships between UCS and NPI have been recommended by several investigators from Japan and Turkey. In the establishment of these relationships, NP tests have been conducted using the same penetrometer and the needle manufactured in Japan. These empirical relations are recommended by: Okada et al. (1985) based on the test results from mudstone and artificial cement-based samples; Takahashi et al. (1988) from sandstone, mudstone, conglomerate, greywacke and tuff; Uchida et al. (2004) from

Ariake clay and sandstone separately; Yamaguchi et al. (1997) from pyroclastic flow and fall deposits; Aydan (2012) and Aydan et al. (2013) from tuff, sandstone, pumice, limestone and lignite measures. The empirical relations recommended by the above-mentioned researchers are given in Table 1, along with the corresponding rock types and the respective references. However, the equations based on utilizing data from artificial materials and soils (i.e., clay, embankment materials) are excluded from the table as this suggested method is only intended to cover NP test in weak and soft rock. Despite that some data come from artificial materials, Okada et al. (1985)'s equation fundamentally is based on mudstone and also used by the manufacturer of the testing device.

Empirical relationships between tensile strength, Young's modulus, P-wave velocity, cohesion, friction angle and S-wave velocity and NPI have also been recommended by Aydan (2012) and Aydan et al. (2013). In the establishment of these relationships, which are given in Table 1, NP tests have been conducted on different types of weak rock using the same penetrometer and needle manufactured in Japan.

7.1.2 Estimation of the Weathering Degree

Hachinohe et al. (1999) described the degree of weathering using the residual strength ratio (R_s), which is the ratio of NPI of the weathered part to that of fresh (unweathered) part of rock cores.

$$R_s = \left(\mathrm{NPI}/\mathrm{NPI}_{fp}\right) \times 100 \qquad (2)$$

where NPI is the measured value and NPI_{fp} is an average value for the fresh part of each drill core. Based on the relationship between R_s and the depth from the bedrock surface, these researchers indicated that R_s decreases with increases in the weathering degree and that the longer the weathering time, the larger is the decrease in R_s. Hachinohe et al. (1999) determined R_s values from Tertiary sandstone and mudstone from the bedrock of marine terraces in Boso Peninsula, Japan. Recently, Aydan et al. (2013) correlated the degree of weathering of soft rocks utilizing the ratio of NPI values of weathered and unweathered soft rocks in a more quantitative manner.

7.2 Rate of Penetration

Various rates of penetrations have been adopted to record the data presented in this document. JGS suggests needle penetration rate of 20 ± 4 mm/min (0.33 ± 0.067 mm/s) (JGS 2012). Ulusay and Erguler (2012) conducted manual tests at rates of penetration ranging from 12 to 264 mm/min and showed that the rate of penetration had no effect on the NPI. Aydan et al. (2013) performed well-controlled NP tests with the help of a compressive machine at 1.2–12 mm/min and observed that the NPI gradually increases as the penetration also increases. Nevertheless, the increase in NPI was small (always <5 N/mm). All these series of tests show that the effect of the needle penetration rate on the NPI is negligible.

7.3 Effect of Needle Geometry

Delft researchers (Ngan-Tillard et al. 2011) conducted five tests using six different types of needles on the same block sample and observed no trend in the peak resistance to penetration as function of needle diameter or cone angle. The tests were conducted on a calcarenitic sample composed of crushable grains of silt and fine sand with no mud between grains. The needles having a diameter varying between 1 and 1.4 mm and a short cone with an angle between 60° and 180° were pushed at a constant penetration rate and the required force was recorded. The peak resistance was defined as the maximum force registered during penetration divided by the cone area. The six needles progressed in the calcarenite by a punch through failure mechanism associated with grain crushing, which explains the insensitivity of the peak resistance to the needle shape and size.

Ngan-Tillard et al. (2012) conducted NP tests with needles with short and long tapered cones noticing a large influence of the slenderness of the needle on the degree of damage caused by the needle and its resistance to buckling. The comparison made by these researchers between the damage caused by the Maruto and modified Eijkelkamp needles is illustrated in Fig. 6; both (a) and (b) images are at the same scale. The modified Eijkelkamp needle with its short conical head at the extremity of a 1-mm-diameter rod had to fragment and open up strong aggregates (labels 1, Fig. 6b, c) to penetrate into the tuff. During testing, a very high penetration resistance (above 300 MPa) was measured and the needle shaft buckled. However, as the diameter of the Maruto's needle increases gradually from 0.38 to 0.84 mm over several millimeters, it might not have encountered any strong aggregates during penetration but gone through the weaker aggregates/cement/matrix by crushing them. Arrows highlight differences in the extent of the damaged zones. Nevertheless, it must be pointed out that micro cracking does occur when Maruto's needle is pushed adjacent to or near harder mineral grains. It is believed that the dilating cracks sub-parallel to the hole shaft (Fig. 6c) were formed during needle removal as high radial stresses caused by needle insertion were released.

Aydan et al. (2008) used three needles with diameters of 1, 2 and 3 mm with flat-circular ends and reported that there

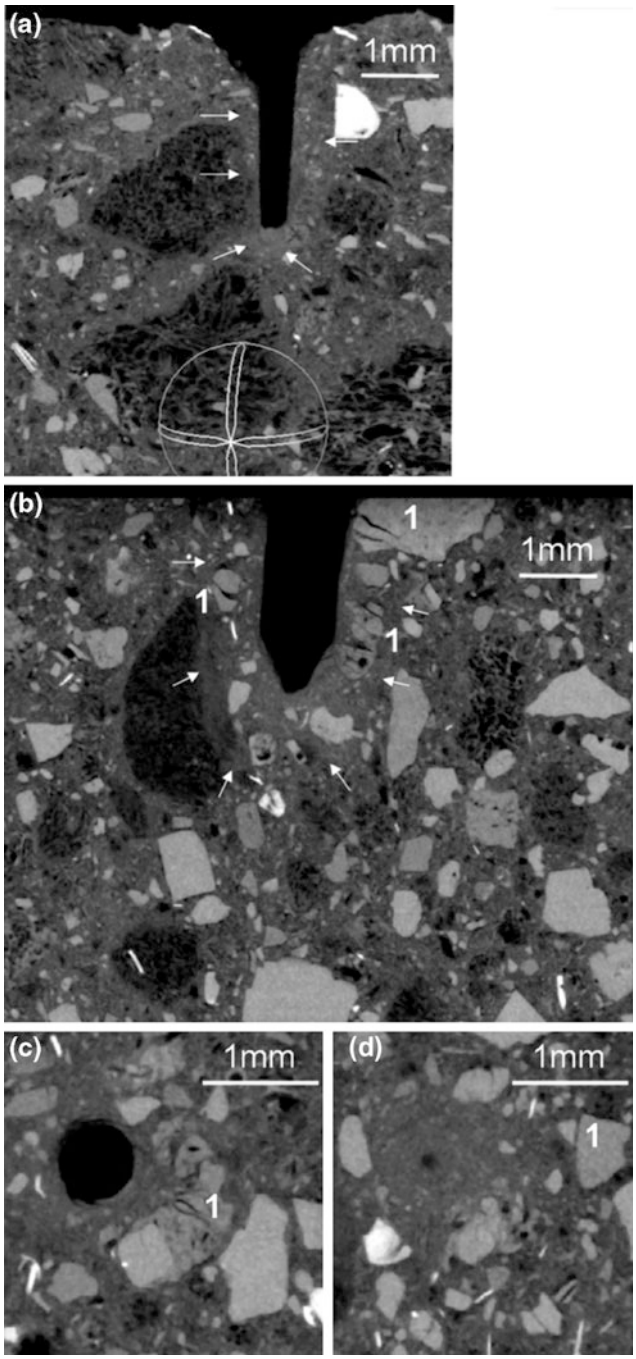

Fig. 6 Micro-CT scans with comparison of damage caused by different needles (*white circle* in the figure is an image rotating tool and was used to make a slice through the 3D micro-CT scanner dataset that passes through the axis of the needle) (Ngan-Tillard et al. 2012)

were some undesirable stress concentrations when the diameter was less than 1 mm and, in this case, non-tapered needles might buckle when high strength rock is tested. The JIS S 3008 (no. 2) needle with a diameter of 0.84 mm was also attached to the load cell and the response measured under the same circumstances. Figure 7 shows an example of measurements for a tuff from Cappadocia, Turkey. If the

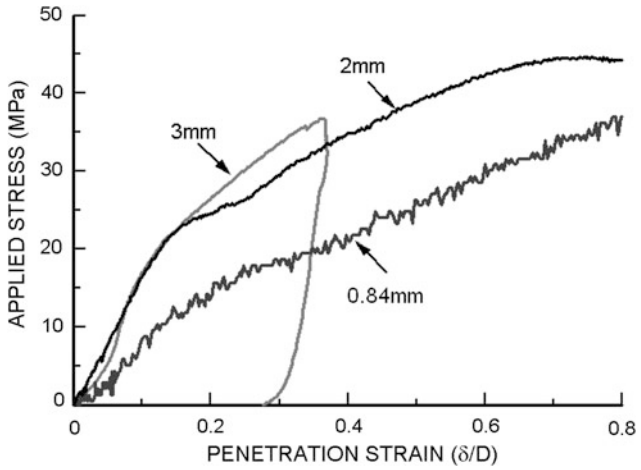

Fig. 7 Comparison of nominal strain versus applied pressure responses by a needle with a diameter of 0.84 mm and 2- and 3-mm flat-ended cylindrical needles (Aydan et al. 2008)

nominal strain is defined in terms of depth of penetration divided by rod diameter, the measured responses prove to be independent of rod diameter. As noted from the responses shown in Fig. 7, the gradient of the penetration curves recorded for both devices is different. The difference results from the plastic response occurring from the very beginning of penetration due to the configuration of the 0.84-mm needle, while the flat end needles initially show an elastic response followed by yielding behavior.

7.4 Influence of Grain Size

The needle penetration tests on various rock types with fine and/or coarse grains showed that scale effects are anticipated when the ratio of grain diameter to needle diameter is smaller than 6–10 (Ngan-Tillard et al. 2012). For these types of coarse-grained rocks, the scatter of NPI values reflects either a low needle diameter to mean grain size, an uneven pore space distribution, or a mixture crushable or less easily crushed grains.

As mentioned by Ngan-Tillard et al. (2009, 2011, 2012) and Ulusay and Erguler (2012), it should be kept in mind that the use of the NP test on rock types such as conglomerate and breccia consisting of coarse hard grains embedded in a cementing material, the test should be limited to infer the properties of the soft matrix.

7.5 Degree of Micro Structural Damage

The penetration of the needle results in a shallow hole at the location of the test. Although it is expected that the damage to rock would be of negligible level, the possible damage

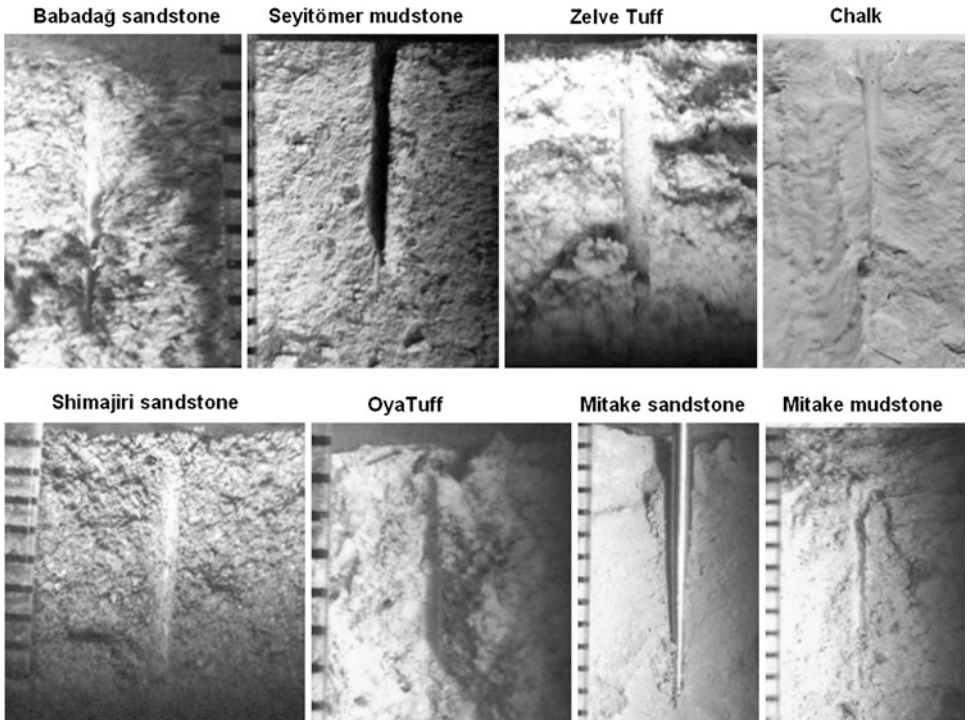

Fig. 8 Views of damage zones in the vicinity of the needle: **a** soapstone; non-polished-no needle (*left*) and non-polished-with needle (*right*); **b** side views of plastic zone formation in split samples of various rocks

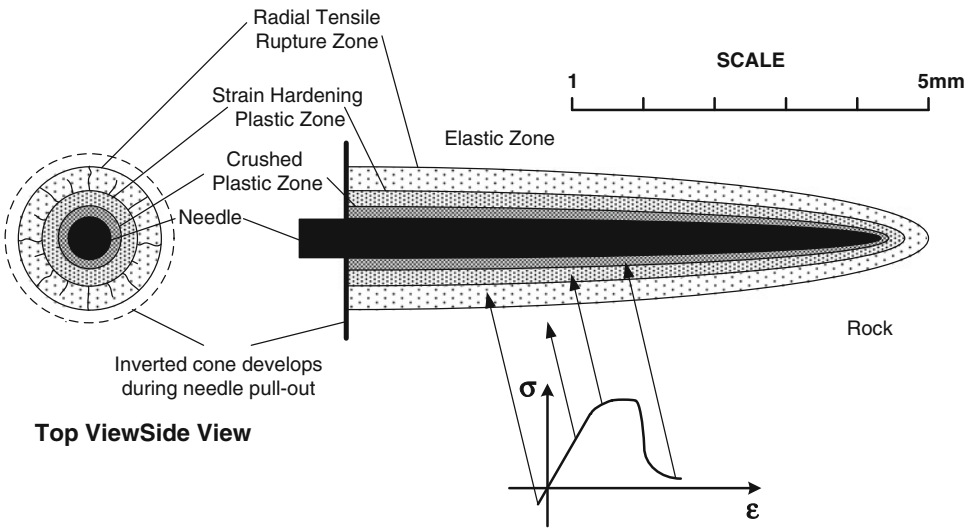

Fig. 9 Illustration of the damage zone around the needle (rearranged from Aydan et al. 2013)

caused by the needle has been investigated by some authors of this suggested method. These researches are briefly summarized in the following sub-sections.

7.5.1 Direct Observation on Damage Zones

Aydan et al. (2013) performed some needle penetration tests on samples of paraffin, chalk, mudstones, tuffs, marls, sandstones and soapstone collected from Turkey and Japan. During experiments, some samples were split so that it was possible to observe the damage zone around the needle. Figure 8 shows several views of damage zones formation in several rocks and materials. Particularly, the damage zones around the needle are clearly differentiated with a sharp color difference in soapstone and paraffin. Aydan et al. (2013) depicted the damage zone as illustrated in Fig. 9. There is no doubt that a radially fractured zone occurs particularly in brittle rocks and expands until the penetration depth exceeds the diameter of the needle. However, a compressive (shear) stress-induced plastic zone (strain hardening and crushed zones) develops next to the needle, which is surrounded by a radial tensile fracture zone. Radial tensile fractures may sometimes be invisible when the needle is totally withdrawn. For example, when the plastic zone develops, the initially semi-transparent paraffin and

soapstone become whitish. The radius of the plastic zone seems to be about two to three times the radius of the needle. Furthermore, radial tensile fractures, which occur beforehand, are well distinguished during penetration and one can easily see the development of the inverted cone of material at the close vicinity of the surface. However, the formation and extension of tensile radial fractures gradually decrease as the penetration depth increases. When rocks have low density such as in mudstone, the formation of tensile fractures is almost suppressed. On the other hand when rocks become denser like soapstone whose unit weight is about 27 kN/m^3 and porosity <1 %, the formation of tensile cracks becomes quite dominant in the overall process. Particularly, post-yielding behavior is also another major parameter in damage zone formation. If post-yielding is ductile, tensile fracture formation becomes suppressed while it is vice versa when the post-yielding is brittle.

7.5.2 CT Scanning Observations on Damage Zone

Ngan-Tillard et al. (2012) investigated the effect of damage caused by needle penetration using X-ray micro-tomography and environmental scanning electronic microscopy after the withdrawal of the needle (Figs. 10 and 11). They tested mudstone, marl and tuff samples from Turkey and calcarenite sample from the Netherlands. They showed that all failure patterns are concentrated around the needle hole. For all rocks the failure patterns consist of a compaction zone ahead and along the needle hole. For some rocks, other types of failure are also discerned. Densification around the hole is clearly visible in porous rocks containing crushable grains (marl, calcarenite and tuff). During needle penetration test, a punch-through mechanism associated with crushing rather than grain debonding takes place. Fine-grained materials (fines) are produced and compacted by the passage of the needle. In the tuff sample, while pumice is reduced to powder, less crushable grains made of quartz and plagioclase minerals are split in the radial direction. In the mudstone, the most brittle of the tested materials by Ngan-Tillard et al. (2012), dilating cracks initiating at the needle tip and propagating toward the free surface of the sample, away from the needle shaft, are also visible on micro-CT scans. They deepen the large crater observed at the point of impact on the core surface. The post-test observations do not allow the sequence of the different failure mechanisms taking place to be established. Spalling, i.e., detachment of plate-shaped slabs from the needle hole, is also observed. It is thought to have occurred during unloading and needle retrieval when the high radial confining stresses generated by needle penetration were released. Ideally, the sequence of events should have been tracked by conducting in vivo X-ray micro-tomography tests during needle loading, unloading and retrieval. Unfortunately, the needle creates metal artefacts on the micro-CT scans that hide subtle deformation patterns.

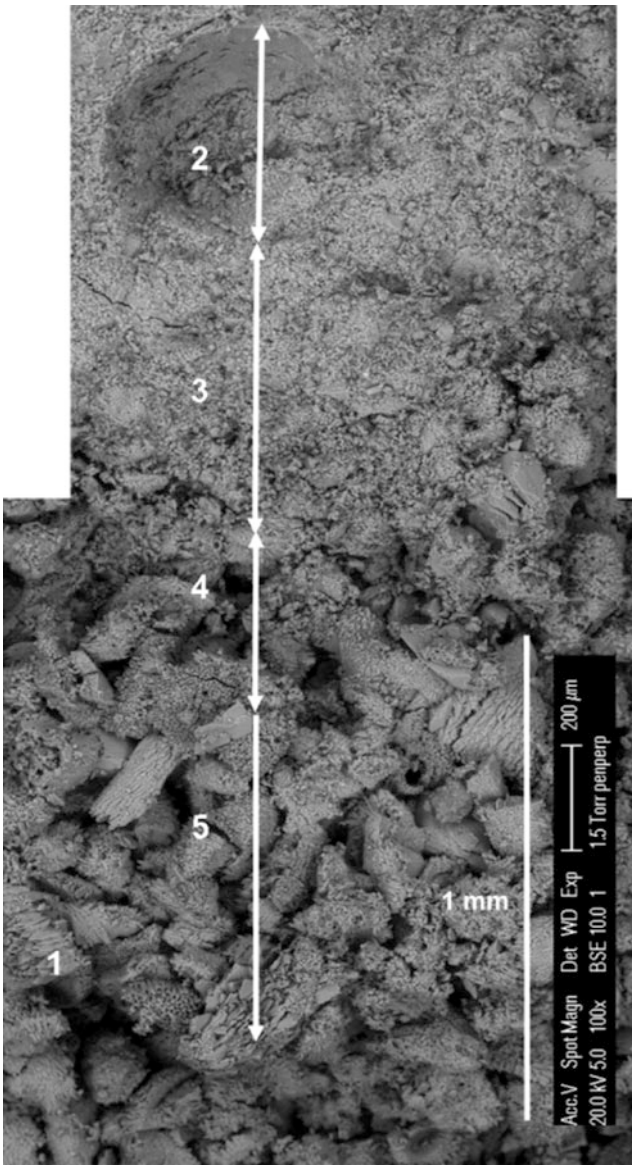

Fig. 10 ESEM photographs of the calcarenite nearby a hole at 100 magnification: *1* bioclast covered by a fringe of dog-teeth calcite cement, *2* imprint of needle tip, *3* crushed zone, *4* transition zone, *5* intact zone (after Ngan-Tillard et al. 2012)

Aydan et al. (2013) used the same X-ray micro-tomography technique to check the effect of additional damage zone formation by the withdrawal procedure. The penetration depths of the needle were set at 2.5, 5.0, 7.5 and 10.0 mm. For soapstone and mudstone samples, the formation of damage zones around the needle was investigated using the μ-focus X-ray CT Scanner System before and after the withdrawal of the needles. Figure 12 shows some selected images of these experiments. Aydan et al. (2013) concluded that the force to be applied to the needle might be up to 40–50 N during the withdrawal procedure, which reverses the stress conditions around the needle and

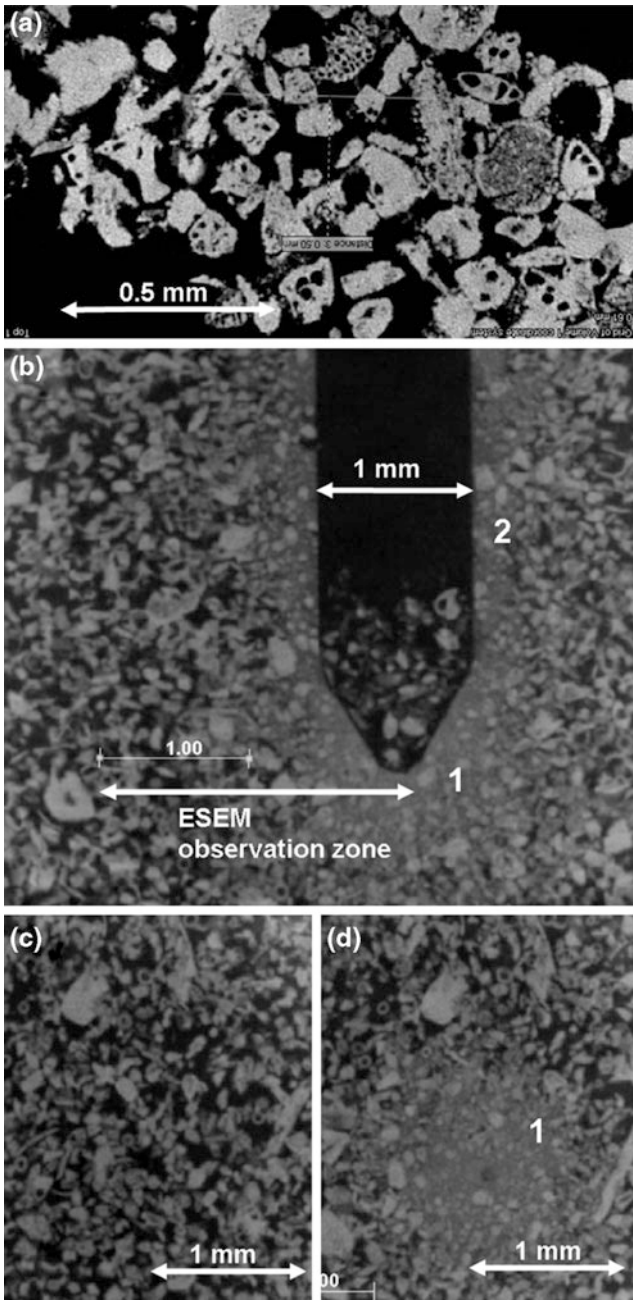

Fig. 11 Micro-CT images of the calcarenite: **a** details of the microstructure showing a large variety of bioclasts (resolution: 0.0018 mm), **b–d** micro-CT scans before and after testing with the modified Eijkelkamp NP in a 10-mm-diameter core (resolution: $0.007 \times 0.007 \times 0.007$ mm^3; **b** section parallel to the needle shaft. Zone ahead of the needle tip: **c** before and **d** after needle penetration and retrieval (note the extent of the zone observed with the ESEM). *1*, *2* crushed compacted zones (after Ngan-Tillard et al. 2011)

causes some additional damage around the needles. Some of the inverted cone-like cracking is a consequence of this process. Despite some interference caused by the needle, damage zones are observed mainly in the mudstone and tensile fractures are observed mainly in the soapstone. As for the damaged zone of the mudstone, it occurs as shown in the schematic model in Fig. 8. It is also found that as expected, the damaged zone becomes larger around the tip of the needle. This is because of the large compression stress during the process of penetration. Furthermore, the withdrawal of the needle definitely caused formation of new fractures or extended the previously formed cracks. However, the tangential cracks close after needle withdrawal.

7.6 Influence of Water Content

Soft and weak rocks containing water-absorbing minerals are generally prone to water content variations, which can drastically change their mechanical properties (Aydan and Ulusay 2003, 2013). The value of needle penetration index (NPI) is expected to decrease as rock water content increases, as reported by Aydan (2012). He also examined the correlations among various engineering properties with needle penetration index (NPI) as a function of water content as shown in Fig. 13 for Oya tuff. The relations established for engineering properties of soft rocks as a function of saturation are basically found to be the same for NPI.

Nakamura and Sasaki (1991) reported a linear relationship between porosity of soft and weak rocks, such as the Tertiary mudstone, sandstone, tuff and conglomerate, and dry/saturated strength ratio (Fig. 14). Therefore, it would be possible to estimate the reduction of engineering properties of soft and weak rocks from the variation of needle penetration index with saturation.

7.7 Variation of NPI with Thawing–Freezing and Drying–Wetting Cycles

It is well known that the properties of rocks deteriorate with the number of thawing–freezing and drying–wetting cycles. The needle penetration index value is expected to decrease with increasing number of these cycles. Figure 15 shows the variation of NPI with the number of drying-wetting cycles for Oya tuff. As noted from the figure, the value of NPI gradually decreases and, therefore, NPI may also be used to assess the degradation of soft rocks subjected to freezing and thawing and drying–wetting cycles.

7.8 Elasto-Plastic Characteristics

Aydan et al. (2008) also explored the use of flat-tip needles to infer the elasto-plastic characteristics of rocks from a single experiment. For this purpose, the diameter of flat-tip

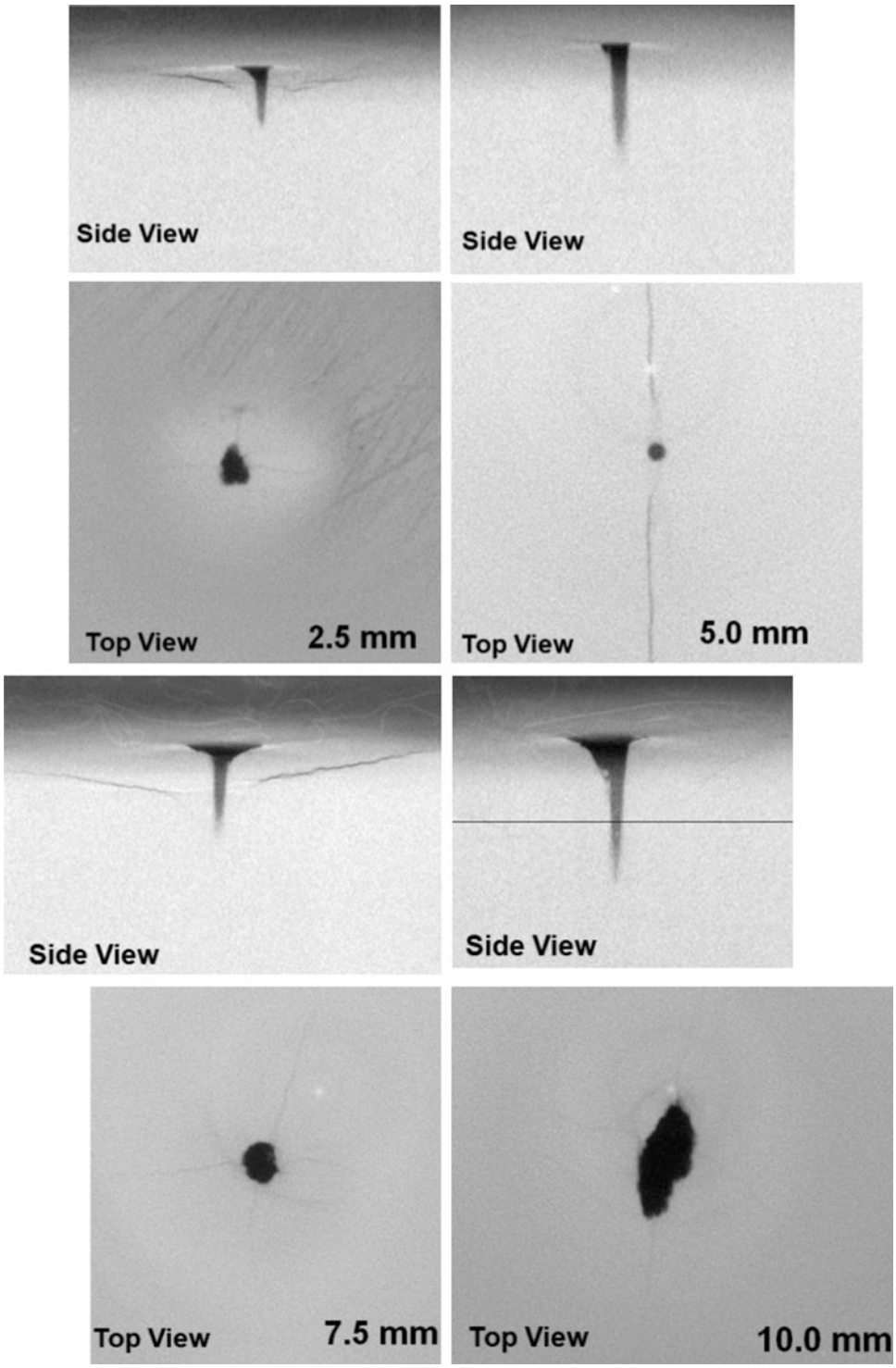

Fig. 12 Some selected images obtained from X-ray micro-CT scanning of soapstone (Saitama and Gifu, Japan) at penetration depths of 2.5, 5.0, 7.5 and 10.0 mm. *Dark zones* correspond to fractures and permanent shape of hole after needle withdrawal. *Dark thin lines* in *top* views are tensile fractures. Dish-like truncated *dark lines* are induced by tensile stresses (Aydan et al. 2013)

needles varied and their responses investigated. Some theoretical and numerical methods were used to infer the properties of rocks from the responses measured by this special experimental technique. Using a theoretical model it was possible to determine the yield function constants such as tensile strength, uniaxial compressive strength, friction angle and deformability parameters such as elastic modulus and Poisson's ratio from a single experiment (Fig. 16).

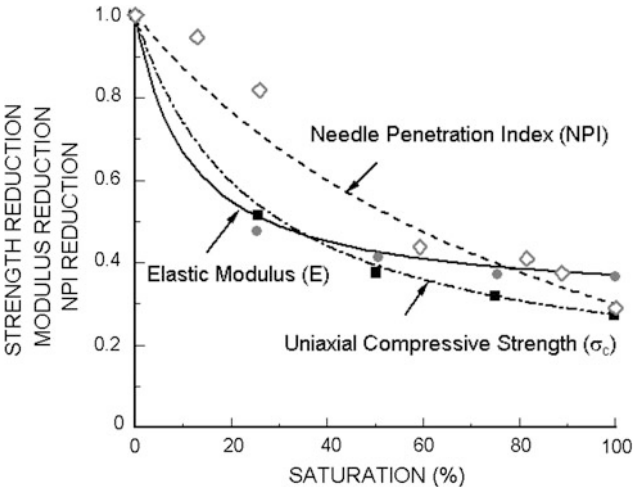

Fig. 13 Variation of normalized elastic modulus (*black dots*) and uniaxial compressive strength (*black squares*) and needle penetration index (NPI) (*open diamonds*) in relation to saturation (Aydan 2012)

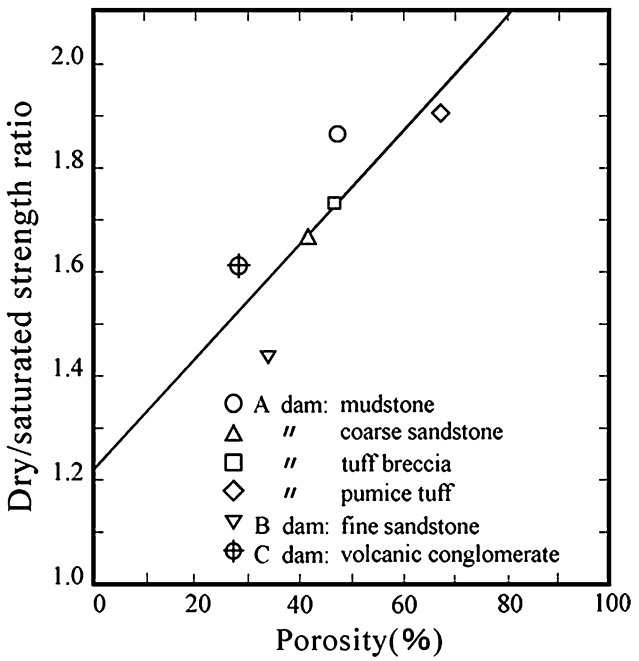

Fig. 14 Relationship between porosity or rocks and dry/saturated NPI strength ratio (Nakamura and Sasaki 1991)

7.9 Time-Dependent Properties

Aydan et al. (2011) devised an experimental setup with a 3-mm flat-tip needle to investigate creep characteristics of rocks. This type of creep experiments is also known as impression creep experiments and are relatively easy to perform; the capacity of loading equipment is relatively small compared to conventional creep experiments. Recently, Aydan et al. (2013) carried out needle penetration

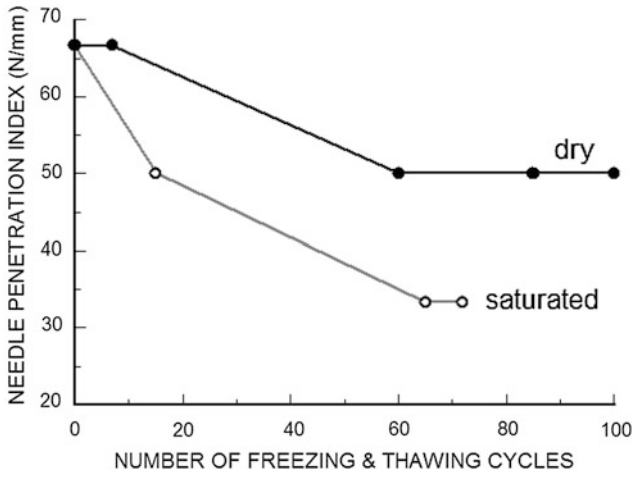

Fig. 15 The variation of NPI with the cycle number of thawing–freezing for Oya tuff (Aydan 2012)

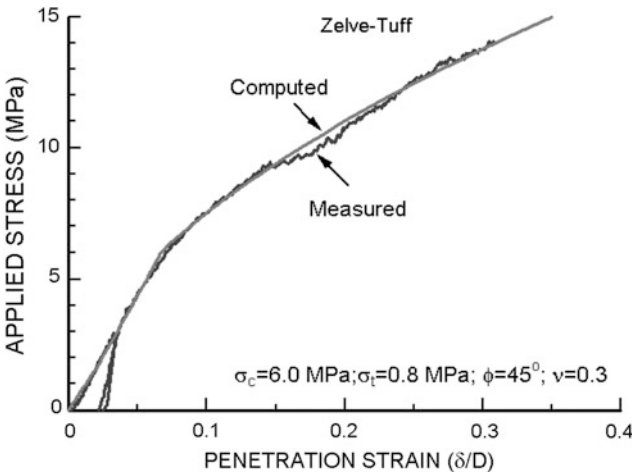

Fig. 16 Comparison of computed and measured nominal strain versus applied pressure responses (δ penetration; D diameter (from Aydan et al. 2008)

tests to investigate both relaxation and creep characteristics of some soft rocks and found similar results to those from specific relaxation and creep experiments. Such experiments to investigate the time-dependent characteristics may be a further possible application of the needle penetration test. However, it should be noted that, for such purpose, the needle penetrometer has to be equipped with continuous monitoring devices for measuring both the load and penetration depth.

Acknowledgments The authors acknowledge the doctorate student of Ömer Aydan, M. Yagi from the Graduate School of Science and Engineering, Tokai University, for his help on the direct observation of damage in rock samples caused during the needle penetration tests. The authors also acknowledge the three reviewers (Prof. Hanifi Çopur, Dr. Yoshikazu Yamaguchi and Dr. Peter N.W. Verhoef) and the two members of the ISRM Commission on Testing Methods (Dr. Jose Muralha and

Prof. Hasan Gerçek) for their critical reviews and constructive comments that led to significant improvements to the Suggested Method. In addition, the authors sincerely thank Prof. Sergio Fontoura, the member of the Commission, for his kind help throughout the review process of the Suggested Method.

References

Aydan Ö (2012) The inference of physico-mechanical properties of soft rocks and the evaluation of the effect of water content and weathering on their mechanical properties from needle penetration tests. Symposium of ARMA, Chicago, Paper No. ARMA12-639 (on CD)

Aydan Ö, Ulusay R (2003) Geotechnical and geoenvironmental characteristics of man-made underground structures in Cappadocia, Turkey. Eng Geol 69:245–272

Aydan Ö, Ulusay R (2013) Geomechanical evaluation of Derinkuyu Antique underground City and its implications in geoengineering. Rock Mech Rock Eng 46:731–754

Aydan Ö, Seiki T, Ito T, Ulusay R, Yüzer E (2006) A comparative study on engineering properties of tuffs from Cappadocia of Turkey and Oya of Japan. In: Proceedings of the Symposium on Modern Applications of Engineering Geology, Turkish National Group of Engineering Geology, Denizli, pp 425–433

Aydan Ö, Watanabe S, Tokashiki N (2008) The inference of mechanical properties of rocks from penetration tests. In: Majdi A, Ghazvinian A (eds) Proceedings of the 5th Asian Rock Mechanics Symposium (ARMS5), Tehran, Iran, vol 1, pp 213–220

Aydan Ö, Rassouli F, Ito T (2011) Multi-parameter responses of Oya tuff during experiments on its time-dependent characteristics. In: Proceedings of 45th US Rock Mechanics/Geomechanics Symp., San Francisco, ARMA 11-294

Aydan Ö, Sato A, Yagi M (2013) The inference of geo-mechanical properties of soft rocks and their degradation from needle penetration tests. Rock Mech Rock Eng. doi:10.1007/s00603-013-0477-5

Erguler ZA, Ulusay R (2007) Estimation of uniaxial compressive strength of clay-bearing weak rocks using needle penetration response. In: Proceedings of 11th Congress on Int. Soc. Rock Mechanics, Lisbon, vol 1, pp 265–268

Hachinohe S, Hiraki N, Suzuki T (1999) Rates of weathering and temporal changes in strength of bedrock of marine terraces in Boso Peninsula, Japan. Eng Geol 55:29–43

ISRM (2007) The complete ISRM suggested methods for rock characterization, testing and monitoring: 1974–2006. In: Ulusay R, Hudson JA (eds) Suggested methods prepared by the commission on testing methods, International Society for Rock Mechanics, Compilation Arranged by the ISRM Turkish National Group, Kozan Ofset, Ankara, Turkey

JGS (Japanese Geotechnical Society) (2012) Method for needle penetration test (JGS: 3431-2012). Japanese standards and explanations of geotechnical and geoenvironmental investigation methods, no. 1, JGS Publication, Tokyo, pp 426–432 (in Japanese)

JSCE (Japan Society of Civil Engineers) (1991) A suggested method for investigation and testing of soft rocks. Committee on Rock Mechanics of JSCE, p 124 (in Japanese)

JSCE-RMC (1980) A suggested method for investigation and testing of soft rocks. In: Japan Society of Civil Engineers, Rock Mechanics Committee, The 4th Sub-committee, Tokyo (in Japanese)

Nakamura Y, Sasaki Y (1991) Simple test for rock mass classification of dam foundation. Eng Dams 53:25–37 (in Japanese)

Ngan-Tillard DJM, Verwaal W, Maurenbrecher PM, van Paassen LA (2009) Microstructural degradation of Maastrichtian limestones. In: Proceedings of Eurock 2009, engineering in difficult ground conditions soft rocks and Karst Leiden. CRC Press, pp 321–326

Ngan-Tillard DJM, Verwaal W, Mulder A, Engin HK, Ulusay R (2011) Application of the needle penetration test to a calcarenite, Maastricht, the Netherlands. Eng Geol 123:214–224

Ngan-Tillard DJM, Engin HK, Verwaal W, Mulder A, Ulusay R, Ergüler Z (2012) Evaluation of micro-structural damage caused by needle penetration testing. Bull Eng Geol Environ 71(3):487–498

Okada S, Izumiya Y, Iizuka Y, Horiuchi S (1985) The estimation of soft rock strength around a tunnel by needle penetration test. J Jpn Soc Soil Mech Found Eng 33(2):35–38 (in Japanese)

Park Y, Obara Y, Kang SS (2011) Estimation of uniaxial compressive strength of weak rocks using needle penetrometer. In: Qian Q, Zhou Y (eds) Proceedings of 12th ISRM International Congress on Rock Mechanics, Beijing, pp 795–798

PWRI (Public Works Research Institute) (1987) Draft manual of simple tests for rock mass classification of dam foundation on soft rocks, Technical note of PWRI, No. 2506, p 31 (in Japanese)

Takahashi K, Noto K, Yokokawa I (1988) Strength characteristics of Kobe formation in Akashi Strata (No. 1). In: Proceedings of 10th Japan National Conf. on Geotech. Eng., The Japanese Geotechnical Society, pp 1231–1232 (in Japanese)

Uchida N, Etoh Y, Ono H, Miura N (2004) Strength evaluation of deep mixing soil–cement by needle penetration test. J Jpn Soc Soil Mech Found Eng 52(7):23–25 (in Japanese)

Ulusay R, Erguler ZA (2012) Needle penetration test: evaluation of its performance and possible uses in predicting strength of weak and soft rocks. Eng Geol 149–150:47–56

Yamaguchi Y, Ogawa N, Kawasaki M, Nakamura A (1997) Evaluation of seepage failure response potential of dam foundation with simplified tests. J Jpn Soc Eng Geol 38(3):130–144